International Journal of Nanomedicine

Dovepress
open access to scientific and medical research

Open Access Full Text Article

ORIGINAL RESEARCH

Chitosan-polyvinyl alcohol nanoscale liquid film-forming system facilitates MRSA-infected wound healing by enhancing antibacterial and antibiofilm properties

This article was published in the following Dove Press journal:
International Journal of Nanomedicine

Sha Yang*
Yun Yang*
Sixin Cui
Ziqi Feng
Yuzhi Du
Zhen Song
Yanan Tong
Liuyang Yang
Zelin Wang
Hao Zeng
Quanming Zou
Hongwu Sun

National Engineering Research Center of Immunological Products & Department of Microbiology and Biochemical Pharmacy, College of Pharmacy, Third Military Medical University of Chinese PLA, Chongqing, 400038, People's Republic of China

*These authors contributed equally to this work

Correspondence: Quanming Zou; Hongwu Sun
National Engineering Research Center of Immunological Products, Department of Microbiology and Biochemical Pharmacy, College of Pharmacy, Third Military Medical University of Chinese PLA, 30 Sha Ping Ba Gaotanyan Street, Chongqing, 400038, People's Republic of China
Tel/fax +86 23 6875 2377
Email qmzou2007@163.com; sunhongwu2001@163.com

Introduction: Methicillin-resistant *Staphylococcus aureus* (MRSA) is one of the most predominant and fatal pathogens at wound infection sites. MRSA is difficult to treat because of its antibiotic resistance and ability to form biofilms at the wound site.

Methods: In this study, a novel nanoscale liquid film-forming system (LFFS) loaded with benzalkonium bromide was produced based on polyvinyl alcohol and chitosan.

Results: This LFFS showed a faster and more potent effect against MRSA252 than benzalkonium bromide aqueous solution both in vitro and in vivo. Additionally, the LFFS had a stronger ability to destroy biofilms (5 mg/mL) and inhibit their formation (1.33 μg/mL). The LFFS inflicted obvious damage to the structure and integrity of MRSA cell membranes and caused increases in the release of alkaline phosphate and lactate dehydrogenase in the relative electrical conductivity and in K^+ and Mg^{2+} concentrations due to changes in the MRSA cell membrane permeability.

Conclusion: The novel LFFS is promising as an effective system for disinfectant delivery and for application in the treatment of MRSA wound infections.

Keywords: liquid film-forming system, methicillin-resistant *Staphylococcus aureus*, wound healing, antibiofilm, antibacterial

Introduction

Wound healing has always been an important topic in medicine and biology, and thus, an area of interest for many years.[1] Once a wound occurs, the normal function of the skin is disrupted due to the incomplete anatomical structure and natural defense barriers, and microorganisms can thereupon easily invade and infect the wound site.[2] This issue has become a major public health care burden accounting for more than 25 billion dollars in costs annually.[3] Wound healing is crucial for restoring the functional status and anatomical continuity of skin tissue.[2] Delayed healing is the most challenging problem in wound management, and bacterial contamination is a major obstacle to the wound-healing process.[4] Many antimicrobial agents are available, including silver sulfadiazine, polymyxin B sulfate, gentamycin, neomycin, and bacitracin, and these agents are widely applied to treat wound infections. However, when applied in common topical forms, such as ointments and gels, these agents barely perform in practical applications because they are easily wiped from wound exposure sites.[5] Thus, a novel suitable formulation for wounds is vital.

Methicillin-resistant *Staphylococcus aureus* (MRSA) is of particular concern because of the limited treatment measures available for treating MRSA wound

submit your manuscript | www.dovepress.com
Dovepress
http://dx.doi.org/10.2147/IJN.S161680

infections.[6] MRSA has become a leading cause of wound infection and is not easily eradicated by routine antimicrobial therapies, making MRSA outbreaks a worldwide problem in recent decades, especially in the developing world. Moreover, biofilms, which are commonly present at wound infection sites, formed by MRSA can delay wound healing and resist the therapeutic efficacy of conventional antibiotics.[7] Therefore, a novel and effective therapy to treat MRSA wound infections is urgently needed.

Benzalkonium bromide (BZL), a well-known quaternary ammonium compound, is a common cationic surfactant widely utilized in industrial and medical applications, including as a sanitizer, a fungicide, an antiseptic, a disinfectant, and an emulsifier.[8] Our previous studies have shown that BZL can effectively inhibit MRSA, and the compound is currently in the form of a foam, a sponge, and a hydrogel to optimize its pharmaceutical properties in topical administration. However, the drug retention times of the above formulations at the wound site are too short to play an efficient role in MRSA eradication.[9] Therefore, a suitable delivery system containing BZL for wound healing is necessary in clinical applications.

Liquid film-forming systems (LFFSs) are ideal for this situation because of the following advantages: enhanced therapeutic efficacy and wound-healing activity, reduced side effects, and minimized administration frequency.[9] Polyvinyl alcohol (PVA) is widely used in film preparation for its excellent biodegradable properties and low toxicity.[10] PVA 0588 is the only PVA derivative that has been approved by the China Food and Drug Administration for biomedical applications and is attracting increasing attention due to its optimal biocompatibility and unique mechanical properties.[11] Studies have shown that biomimetic material, chitosan (CS), loaded with antibiotics can prolong drug residence time and prevent injury, thereby lessening infections in wound tissues. Furthermore, films made of CS have been used extensively in drug delivery systems and tissue engineering scaffolds due to their biodegradability, biocompatibility, and low toxicity.[12] To date, however, an LFFS fabricated with CS and PVA for use as a BZL delivery system has not been reported.

In this manuscript, we designed a novel BZL-containing LFFS that is fabricated with CS and PVA 0588. We hypothesize that this LFFS can promote wound-healing treatment with excellent antibacterial efficacy and a delayed release effect (Figure 1). Most importantly, this LFFS has an outstanding ability to eradicate or inhibit biofilms and to destroy the structural integrity of the bacterial cell membrane.

Materials and methods

Bacterial, animals, and ethics statement

MRSA252 was sourced from the American Type Culture Collection (ATCC, Manassas, VA, USA). Mueller–Hinton broth (MHB), Mueller–Hinton agar (MHA), and tryptic soy broth (TSB) were all purchased from AOBOX Biotechnology (Beijing, People's Republic of China). TSB supplemented with 0.5% glucose and 2.0% NaCl was used in biofilm production,[13] and an optical density (OD) of 1.0 at 595 nm was defined as 1×10^9 CFU/mL. BALB/c mice (female, 6–8 weeks

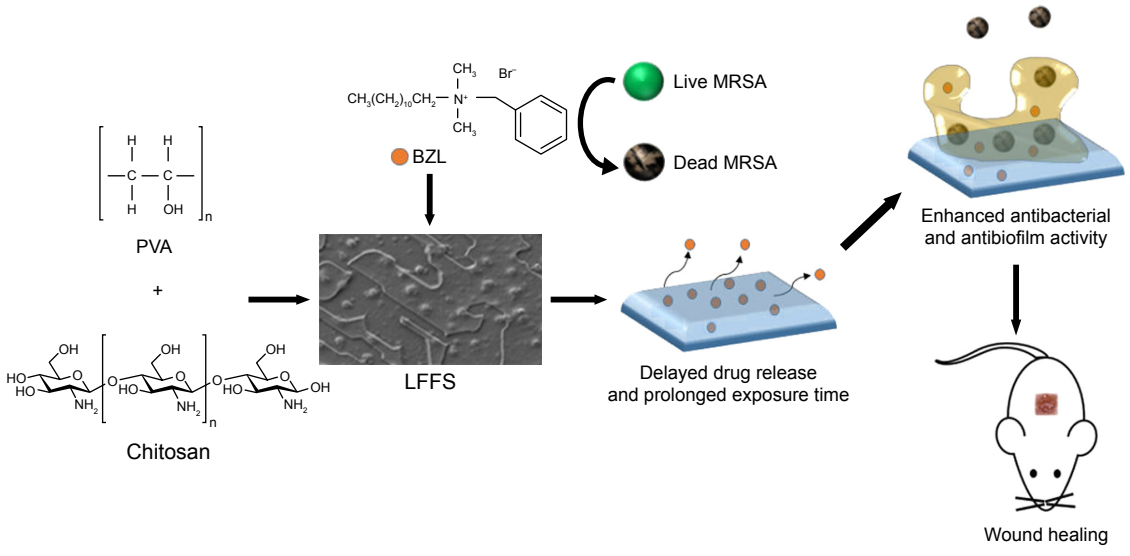

Figure 1 Schematic depiction of the design of the LFFS.
Note: This novel LFFS can promote healing of MRSA-infected wound with excellent antibacterial efficacy, a delayed release effect, and an outstanding ability to eradicate or inhibit biofilms.
Abbreviations: BZL, benzalkonium bromide; LFFS, liquid film-forming system; MRSA, methicillin-resistant *Staphylococcus aureus*; PVA, polyvinyl alcohol.

old, specific pathogen free) were purchased from Beijing HFK Bioscience Co. Ltd. (Beijing, People's Republic of China). Animal testing was approved by the Laboratory Animal Welfare and Ethical Committee of Third Medical Military University of the Chinese People's Liberation Army and was performed in accordance with the Guide for the Care and Use of Laboratory Animals. To minimize suffering, all mice that underwent surgery were treated with isoflurane anesthesia.

Design and preparation of a series of film-forming systems

The film-forming formation systems were prepared according to our patented technology described previously (Chinese Innovation Patent, No 101879283B), as shown in Table S1. In brief, CS (1%, w/v; low molecular weight: 50–190 kDa; acetylation: 85%; viscosity: 20–200 mPa·s, Sigma-Aldrich Co., St Louis, MO, USA) was dissolved in 1% acetate buffer (pH 4.4). Then, different contents of PVA (average degree of polymerization: 600–800; alcoholysis degree: 88% ± 2%; viscosity: 4–6 mPa·s, Meijia Meng Technology Co., Ltd., Chongqing, People's Republic of China) were prepared by dissolution in hot water (70°C). BZL (5 mg/mL, Yusheng Pharmaceutical, Chongqing, China.) was added to the PVA solution, and the resulting solution was then added to the CS solution with mixing at a speed of 200 rpm for 10 minutes. Then, the mixtures were added dropwise under gentle agitation to observe the transparent and easily flowing film-forming system. The blank film-forming system (BFFS) was prepared using the above methods without the addition of BZL.

Determination of PVA concentration in the film-forming system

Influence of the film morphology

The morphologies of LFFS samples with five different PVA contents (0%, 2.5%, 5%, 7.5%, and 10%) were analyzed with a scanning electron microscope (SEM, S-3400N, Hitachi, Tokyo, Japan) with a step voltage of 10 kV after coating with a 200 Å of gold-palladium layer.

Influence of sustained release in PBS

The release profiles of LFFS samples with different PVA contents (0%, 2.5%, 5%, 7.5%, 10%) were examined in PBS (pH 6.8) at 37°C. In brief, 2 mL of each sample (5 mg/mL) was added to preprocessed dialysis bags (molecular weight cut off: 10,000 g/mol, Sangon Biotech Co., Ltd, Shanghai, People's Republic of China) in 200 mL of PBS. For all samples, the optical densities at 215 nm were measured at 0, 0.167, 0.33, 0.5, 0.75, 1, 1.5, 2, 3, 4, 6, 8, 10, 12, 24, 36, 48, 60, 72, 96, 120, 144, and 168 hours. In addition, considering that the pH value of normal human skin is between 4.0 and 6.0 and that pH at a wound site can rise to approximately 7.0 to 8.0,[14,15] the release profiles of LFFS and BZL were assessed in PBS at different pH values (pH 4.0, 6.0, and 8.0) at 37°C with the previously described methods.

Influence of minimum inhibitory concentrations (MICs)

The MIC was defined as lowest concentration inducing an OD <0.05 at 595 nm after cultivation for 24 hours. According to previous reports,[16] each sample, as listed in the Table S2, was diluted to a BZL concentration with 6.25, 14.3, 25.0, 33.3, 50.0, 66.7, 100, or 200 μg/mL, separately. Next, 20 μL of the above samples and 180 μL of the bacterial suspensions (1.0×10^5 CFU/mL) were added to a 96-well microtiter plate (Costar 3599, Corning Inc., Corning, NY, USA). After cultivation for 24 hours, the OD (595 nm) values of the samples were read by a microplate reader (Bio-Rad 6.0, Bio-Rad Laboratories Inc., Hercules, CA, USA).

Preparation and characterization of the liquid film-forming system (LFFS)

Based on the results of the films morphologies (Figure S1), sustained release profiles (Figure 2A), and antibacterial activities (Table S2) with different concentrations of PVA, we formed the LFFS with 5% PVA, 1% CS, and 0.5% BZL (5 mg/mL) by previously described methods (Chinese Innovation Patent, No 101879283B). Its film-forming ability, morphology, and stability were determined. Briefly, to assess the film-forming ability, 50 μL of LFFS was added to a glass slide, which was then dried in a hot air oven (DGF20022B, Chongqing, People's Republic of China) at 37°C ± 0.5°C. The thickness and maintenance time of the LFFS were visually observed. In addition, the morphology of fresh LFFS samples was observed by an SEM (S-3400N, Hitachi) after the samples were diluted 100-fold and 200-fold in water with a transmission electron microscope (FEI TECNAI10, Philips Electron Optics, Eindhoven, the Netherlands) with operating at a voltage of 120 kV voltage. The morphology was also observed using an atomic force microscope (AFM IPC-208B, Chongqing University, Chongqing, People's Republic of China) over a scanning area of $1,230 \times 1,230$ nm^2 with point-wise scanning. The film parameters for the measurements, namely, kurtosis (Rku) and skewness (Rsk), and three profiles, including mean roughness average (Ra), mean square

roughness (Rq), and mean roughness depth (Rz), were measured and calculated with G3DR software. The pH of the LFFS was measured with a pH meter.

Antibacterial activity of the LFFSs in vitro

MIC and minimum bacterial concentration (MBC)

The MIC of LFFS was determined by previously described methods. LFFS and BZL samples were serially diluted and filtered to various concentrations (0, 11.11, 11.76, 12.5, 13.33, 14.29, 15.38, 16.67, 18.18, 20, 22.22, 25, 28.57, 33.33, 40, and 50 μg/mL). MBC was defined as the lowest concentration permitting no bacterial growth on MHA plates at the highest dilution. To determine the MBC, 5 μL of each sample was added to MHA plates and incubated at 37°C for 24 hours. To prepare the blank controls, the BFFS was similarly diluted to the highest LFFS concentration.

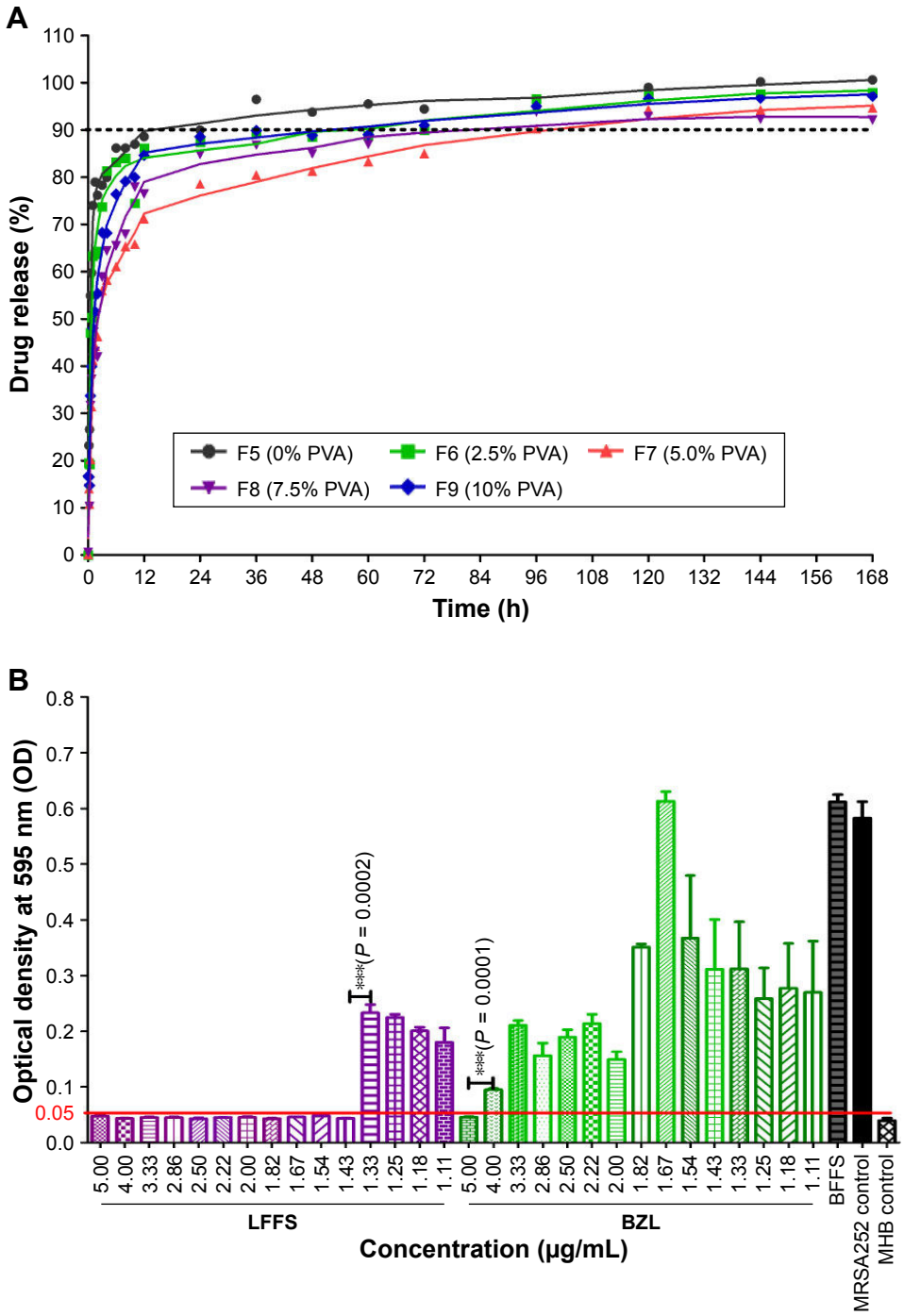

Figure 2 (*Continued*)

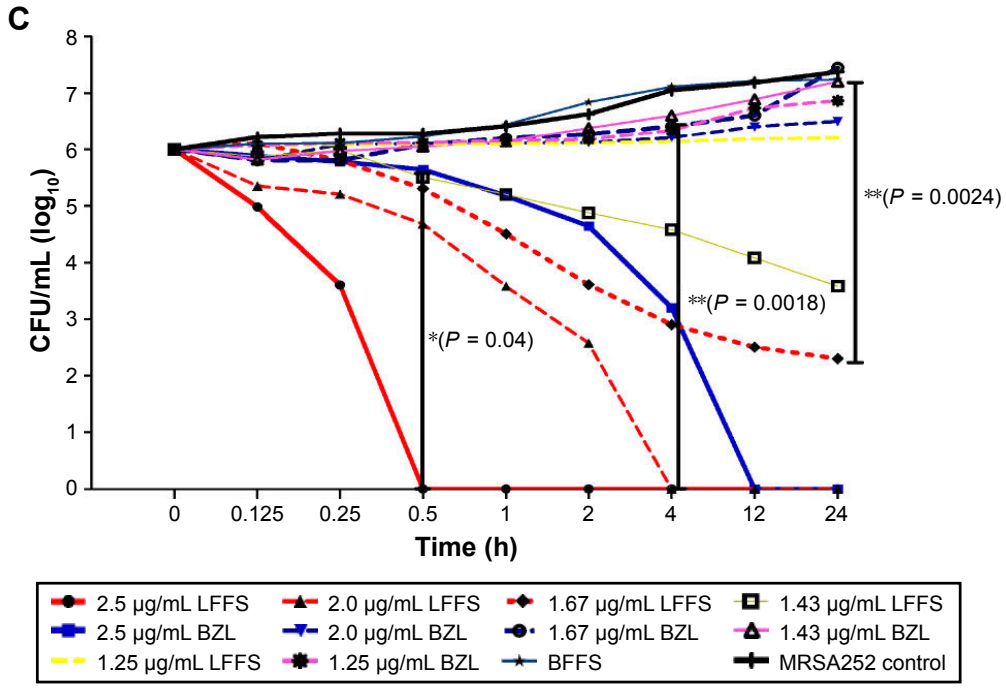

Figure 2 Release profile and antibacterial activity of the LFFS in vitro. (**A**) In vitro release profile of the LFFSs with different PVA contents in PBS. (**B**) MICs. (**C**) Time-kill assay.

Notes: The black line marks a 90% release. Values <0.05 under the OD indicate that bacteria were killed. ***$P < 0.001$ denotes an extremely significant difference, **$P < 0.01$ denotes a highly significant difference, and *$P < 0.05$ denotes a significant difference (n = 3).

Abbreviations: BZL, benzalkonium bromide; CFU, colony-forming unit; F, Formula; LFFS, liquid film-forming system; MHB, Mueller–Hinton broth; MIC, minimum inhibitory concentration; OD, optical density; PBS, phosphate buffer solution; PVA, polyvinyl alcohol.

Time-kill assays

Bacterial cultures (1×10^6 CFU/mL) were incubated for 0, 0.125, 0.25, 0.5, 1, 2, 4, 8, 12, and 24 hours with the LFFS and BZL samples at concentrations of 2.5, 2.0, 1.67, 1.43, and 1.25 μg/mL. After incubation, 5 μL of each specimen was tenfold diluted with MHB (0, 10^1, 10^2, 10^3, 10^4, 10^5, and 10^6), added to MHA plates, and incubated for 24 hours at 37°C. The quantity of bacteria on each plate was calculated with an auto colony counter (Shineso Science & Technology Co., Ltd, Hangzhou, People's Republic of China). As the blank control, the BFFS was diluted to the highest LFFS concentration.

Antibacterial activity of the LFFS in vivo

Experimental design and animal treatment

To examine the skin irritation properties of LFFS and BZL at 5 mg/mL, hair was removed from six mice. Their bare skin was coated with 100 μL of LFFS or BZL (2 mg/mL or 5 mg/mL), BFFS or formalin, and then observed after 1 day. The presence of erythema and edema identified the solution as a skin irritant. In total, 42 mice were divided randomly into 7 groups (n = 6): those treated with LFFS or BZL (5 mg/mL or 2 mg/mL), those with treatment for the BFFS control, or those with wound model and wound infection groups. The dorsal hairs of all mice were removed, and their back skin was subsequently excised to create full-thickness wounds (1.0×1.0 cm^2). After 1 hour, all mice except those in the wound control group were infected with 50 μL of the bacterial suspension (2×10^9 CFU/mL). After 24 hours of infection, all mice except those in the wound infection group and the wound control were processed locally for 14 continuous days. The mice were treated with 50 μL of each solution by applying the skin wound area for 30 seconds twice per day.

Viable bacterial count

At 0, 1, 3, 5, and 7 days after injury, each mouse wound was separately scraped 10 times with a sterile cotton swab. The swabs were placed in 1 mL of sterile saline and agitated to release the bacteria into the liquor. Next, 5 μL of each sample serially diluted 20-fold with sterile saline was applied to MHA plates and incubated at 37°C for 24 hours. The CFUs of every dilution were measured.

Wound-healing study

Open wound areas were documented with a digital camera on days 0, 1, 3, 5, 7, and 14, and the wounds areas in each group were analyzed using ImageJ software. The wound-healing rate was calculated as follows: wound-healing rate (%) = (original

area – unhealed area) ÷ (original area) × 100. The wounds were observed daily, and the wound times including the form scar, completed scar, completed take-off scar, and recovery were recorded for each mouse.

Antibiofilm inhibition and clearance activity

Biofilm formation and clearance ability

MRSA bacterial cultures (1.8 mL, 1×10^7 CFU/mL) were added to 0.2 mL of BZL and LFFS (both with 1.33 μg/mL drug) in each well of a 24-well cell culture plate containing cover slips (Thermo Fisher Scientific, Waltham, MA, USA). The bacteria were incubated for 24 hours at 37°C and washed twice with 0.1 M PBS. For the clearance activity, 2 mL of MRSA252 bacterial cultures (1×10^7 CFU/mL) were grown in 24-well cell culture plates containing cover slips for 24 hours with TSB cultures. The biofilms were washed twice with PBS, and 200 μL of 5 mg/mL BZL and LFFS was added for 8 hours.

Biofilm quantification

After removing the supernatants, wells containing biofilm were washed twice with 1 mL of 0.1 M PBS. Next, 1 mL of absolute ethyl alcohol was fixed for 15 minutes, and the remaining biofilm was stained with 200 μL of crystal violet dye (0.1%) for 10 minutes. The biofilms were washed twice and dissolved with 1 mL of acetic acid (30%). The OD at 570 nm was read with a microplate reader (Bio-Rad Laboratories Inc.).

Examination of biofilm surface structures

Cover slips were fixed with 2.5% glutaraldehyde after removal of the supernatant. The biofilms on the coverslips were treated for SEM observation in a graded series of ethanol. Specimens were viewed via an S-3400N SEM (Hitachi) at an acceleration voltage of 10 kV and a sputter coating with 200 Å of gold palladium.

Examination of biofilm live/dead ratios

The green SYTO-9 (561 nm) probe marked live cells, and the red PI (488 nm) probe marked dead cells. Biofilms were stained with 30 μM propidium iodide (PI) and 6 μM SYTO-9 (LIVE/DEAD 7021 Bacterial Viability Kits; Thermo Fisher Scientific) for 15 minutes at 25°C. A confocal laser scanning microscope (CLSM 780, Zeiss, Oberkochen, Germany) was used to sequentially assess the specimens. The maximum projections of all image stacks were built using ZEN soft (Zeiss), and the green (live) and red areas (dead) in the biofilms were quantified. Additionally, the dead/live ratios and live cell percentages were analyzed.

Inspection of biofilm three-dimensional (3D) structures

The 3D constructions of the biofilms were measured using a high-resolution AFM at Chongqing University (IPC-208B, Chongqing, People's Republic of China) with the following parameters: tungsten-tipped probe with a force constant of 0.06 N/m, imagery acquired in tapping mode, scanning area of $1{,}230 \times 1{,}230$ nm^2, and a point-by-point scanning approach at an indoor temperature. Three profile parameters and two measurement parameters were counted using G3DR software according to previously described methods.

Cell and membrane damage induced by the LFFS

Cell structure imaged by transmission electron microscopy (TEM)

MRSA252 (1×10^6 CFU/mL) cultures were added to LFFS and BZL (1.33 μg/mL), incubated at 37°C, and centrifuged at 6,000× *g* for 5 minutes. After removal of the supernatants, the cells were washed three times with PBS before being treated for TEM observation (FEI TECNAI10, Philips Electron Optics).

Bacterial cell wall integrity

The bacterial cell wall integrity was assessed based on the amount of alkaline phosphatase (AKP) released. MRSA252 (1×10^6 CFU/mL) was added to 1.33 μg/mL LFFS or BZL and incubated at 37°C for 2 and 4 hours before being centrifuged at 6,000× *g* for 5 minutes. AKP levels in the supernatants were examined by AKP kit (A059-1, Nanjing Jiancheng Bioengineering Institute, Nanjing, People's Republic of China).

Bacterial cell membrane integrity

MRSA252 (1×10^6 CFU/mL) cultures were added to 1.33 μg/mL LFFS or BZL and incubated at 37°C for 8 hours in MHB before being centrifuged at 6,000× *g* for 5 minutes. After centrifugation, 5 μL of the supernatants was dissolved in 0.2 mL of sterilized saline and read with a NanoDrop (ND1000, Thermo Fisher Scientific) at 260 nm and 280 nm.

Bacterial cell membrane damage

The lactate dehydrogenase (LDH) index assesses damage to cell membranes. MRSA252 (1×10^9 CFU/mL) cultures were added to 1.33 μg/mL LFFS or BZL and incubated at

37°C for 4 hours with shaking in MHB. Subsequently, the cultures were centrifuged for 5 minutes at 6,000× *g*, and the LDH levels in the supernatants were assessed with an LDH Assay Kit (A020-2, Nanjing Jiancheng Bioengineering Institute) at 2 and 4 hours.

Bacterial membrane permeability

The bacterial membrane permeability was evaluated based on changes in the electrical conductivity of the bacterial culture medium. In brief, MRSA bacteria was centrifuged at 6,000× *g* for 10 minutes after incubation at 37°C for 10 hours. The bacteria were washed and tested with a conductivity apparatus (DDS-307A, Shanghai Precision & Scientific Instrument Co., Ltd, Shanghai, People's Republic of China) with a 5% glucose solution when their electrical conductivities were close to that of 5% glucose and marked as L0. BZL and LFFS solutions at 1.33 μg/mL were added to the bacteria, and the electrical conductivities were measured and marked as L1. These samples were incubated at 37°C for 2 and 4 hours and then measured and marked as L2. The permeability of the cell membrane was calculated according to the following formula: relative electrical conductivity (%) = (L2 − L1) ÷ L0 × 100. Simultaneously, the permeability of the bacterial membranes was measured based on K^+ and Mg^{2+} leakage indicated the permeability of the bacterial membrane. MRSA252 (1×10^9 CFU/mL) cultures were added to LFFS and BZL at 1.33 μg/mL and incubated at 37°C for 4 hours. The cultivations were centrifuged for 5 minutes at 6,000× *g*, and the K^+ and Mg^{2+} ion concentrations in the supernatants were assessed with a potassium assay kit and magnesium assay kit (C001-3, C005) (Jiancheng Bioengineering Institute of Nanjing) at 2 and 4 hours.

Statistical analysis

Statistical analyses were conducted using GraphPad Prism software (version 5.01, GraphPad Software, Inc., La Jolla, CA, USA). Significance is indicated on the graphs by asterisks (*, **, or ***) for *P*-values of 0.05, 0.01, and 0.001, respectively. Student's *t*-tests were used for comparison between two groups, and analysis of variance followed by Tukey's tests were conducted for comparisons among more than two groups.

Results

Determination of PVA concentration in the film-forming system

Ten formations (from F1 to F10) with different contents of PVA or CS were prepared (Table S1), according to our patented technology and previously described method (Chinese Innovation Patent, No 101879283B). In the study on different contents of PVA (F5–F9), we found that F7 (LFFS with 5% PVA) had an incompact and asymmetric morphology that created larger pores with an irregular shape, as it was blocky and straticulate (Figure S1C and H). At 5,000-fold magnification, F5, F8, and F9 (0%, 7.5%, and 10% PVA, respectively) appeared to be in particle states (Figure S1A, D, and E), and F6 (2.5% PVA) showed a dendritic shape (Figure S1B). At 15,000-fold magnification, F8 and F9 exhibited reticular structures (Figure S1I and J), F5 was strip shaped (Figure S1F), and F6 was fusiform (Figure S1G).

The LFFS with 5% PVA (F7) exhibited a distinct sustained release ability compared with the other systems with 0%, 2.5%, 7.5%, and 10% PVA (F5, F6, F8, and F9, respectively) (Figure 2A). The LFFS exhibited a better sustained release capacity than that of the other formulations, as BZL solution needed 45 minutes to reach 90% release, while the LFFS needed 96 hours. The release concentration of F5 reached 90% at 36 hours, while F6, F8, and F9 took 72, 72, and 60 hours to reach 90% release, respectively. Achieving 90% release of BZL took 45 minutes, while the LFFS needed 72, 72, and 90 hours in PBS solutions at pH 4.0, 6.0, and 8.0, respectively, as shown in Figure S2. These data showed that the LFFS exhibited distinct sustained release behavior compared with BZL solution.

The antibacterial effect of F7 (LFFS with 5% PVA) was between 1.75- and 3.49-fold higher than those of F4 (hydrophilic, 0% CS), F6 (2.5% PVA), F8 (7.5% PVA), F9 (10% PVA), F5 (hydrophobic, 0% PVA), and F10 (BZL), as shown in Table S2. In addition, F1 (1% CS), F2 (5% PVA), and F3 (blank LFFS, BFFS) had no antibacterial effect. The MIC values of BZL (5.0 μg/mL) values were 3.49-fold higher than those of LFFS (1.43 μg/mL). Thus, considering the sustained release properties and antibacterial activities of these formulations, we chose F7 (5% PVA) as the optimal LFFS for further experiments.

Antibacterial activity of the LFFS in vitro

The MICs of LFFS against MRSA are shown in Figure 2B and Table S2. Both the MICs and MBCs of the LFFS were 1.43 μg/mL, and those of BZL were 5.00 μg/mL. The MIC and MBCs of BZL against MRSA were 3.49 times higher than those of the LFFS. The time-kill results for the LFFS showed a time- and concentration-dependent effect, as presented in Figure 2C. Consequently, at 2.5 μg/mL, the LFFS displayed a much faster and more potent bactericidal activity than BZL at equivalent times; the LFFS killed all MRSA

bacteria within 0.5 hour, whereas BZL took 12 hours. At 2 μg/mL, the LFFS decreased the bacterial viability by 60% within 2 hours, completely eradicated the bacteria within approximately 4 hours. However, at the same concentration, BZL could not eradicate bacteria within the same time frame (approximately 25% of the bacteria remained alive). Additionally, 1.43 μg/mL LFFS produced a much longer and more stable bacteriostatic effect than BZL at equivalent concentrations. These results reveal that LFFS exhibits a stronger antibacterial effect than BZL on MRSA252 in vitro.

Characterization of the LFFS

The LFFS with 5 mg/mL BZL was transparent and clear (Figure S3A). We can find that a notable thin and difficult-to-remove film was formed in the glass slide after spraying one dip LFFS (Figure S3B). SEM at a magnification of 4,000 reveals that the undiluted sample features a highly smooth surface resulting from interpenetration of the drug into the polymeric network (Figure 3A). The outer layer of the LFFS sample diluted 100-fold with water was smooth, and the inner layer adhered to the pharmaceutical particles, as observed at 50× magnification (Figure 3B). Additional, spherulitic crystallization was decreased because of the miscibility of the drug, resulting in a homogeneous and smooth surface of the solution diluted 100-fold with water at 500× magnification (Figure 3C). The LFFS presented as a reticulate structure at 100-fold dilution and 60,000× magnification by TEM (Figure 3D). At 100,000× magnification, the LFFS displayed a fibrous reticulate structure after 100-fold dilution (Figure 3E) and presented a lamellar structure after 200-fold dilution (Figure 3F). The roughness visible in the AFM images is due to the four-layer lamellar structure of the thickness, and this effect is shown in Figure 3G–I. The Ra, Rz, and Rq of the LFFS were 34.304 ± 11.461 nm, 270.95 ± 205.611 nm, and 40.541 ± 13.856 nm, respectively (Figure S4A), and the Rsk and Rku were 1.392 ± 0.104 and 2.208 ± 0.525, respectively (Figure S4B). The LFFS presented a constant low Rq (~270 nm), which increased as a function of the number of bilayers. LFFS was quite stable and showed no changes in content, phases, drug separation, or precipitation, or any other aspects of unstable appearance after centrifugation (3,000× *g* for 10 minutes).

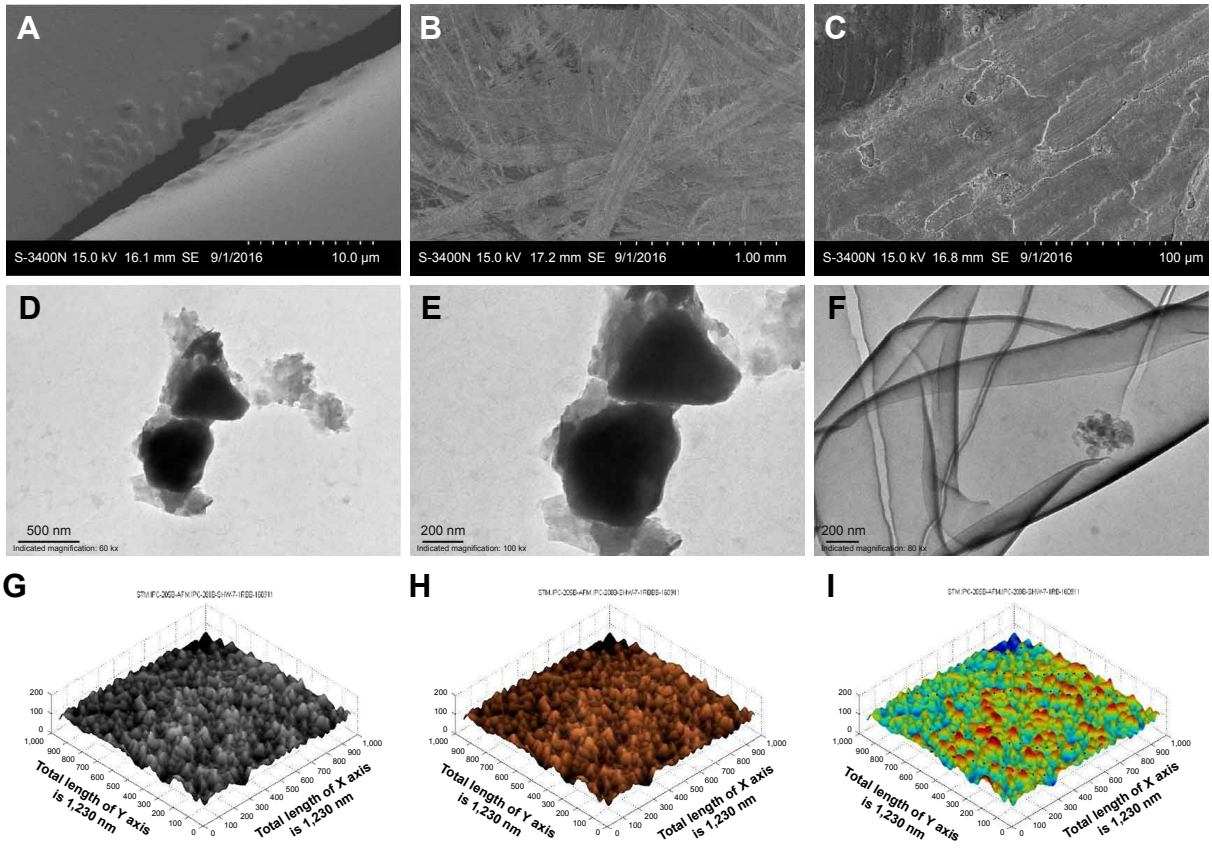

Figure 3 Morphological images of the LFFS obtained by SEM, TEM, and AFM. (**A**–**C**) Morphological SEM images (4,000× magnification, undiluted; 50× magnification, diluted 100-fold with water; 500× magnification, diluted 100-fold with water, respectively). (**D**–**F**) Morphological TEM images (60,000× magnification, diluted 100-fold with water; 100,000× magnification, diluted 100-fold with water; 80,000× magnification, diluted 200-fold with water, respectively). (**G**–**I**) Black scale and grayscale AFM images.
Abbreviations: AFM, atomic force microscope; LFFS, liquid film-forming system; SEM, scanning electron microscope; TEM, transmission electron microscopy.

Antibacterial activity of the LFFS in vivo

The bacterial counts in wounds treated with 5 mg/mL LFFS decreased more rapidly than those in wounds treated with the same concentration of BZL (Figure 4A). By the third day, compared to the initial bacterial counts, the bacterial counts in mouse wounds treated with 5 mg/mL LFFS were decreased by 43% whereas those of the wounds treated with 5 mg/mL BZL were decreased by 27%. On the seventh day, the number of bacteria in wounds treated with 5 mg/mL LFFS were decreased by 81%, whereas the number of bacteria in wounds treated with 5 mg/mL BZL (60%). Similar outcomes were observed in the decreases in the number of bacteria observed after treatment with the LFFS and BZL at 2 mg/mL.

As shown in Figure 4B, the LFFS exhibited a significantly higher healing rate than BZL solution. Wounds treated with 5 mg/mL LFFS showed higher wound-healing rates (78.4%) than those treated with 5 mg/mL BZL (76.82%) on day 7. Furthermore, wounds treated with BFFS (23%) had delayed healing in comparison to those treated with the LFFS and BZL but still exhibited faster healing than those in the model control group (66.03%). On day 14, nearly 100% wound-healing activity was observed in the 5 mg/mL LFFS-treated group, whereas wound-healing rates of 84.7%, 86.82%,

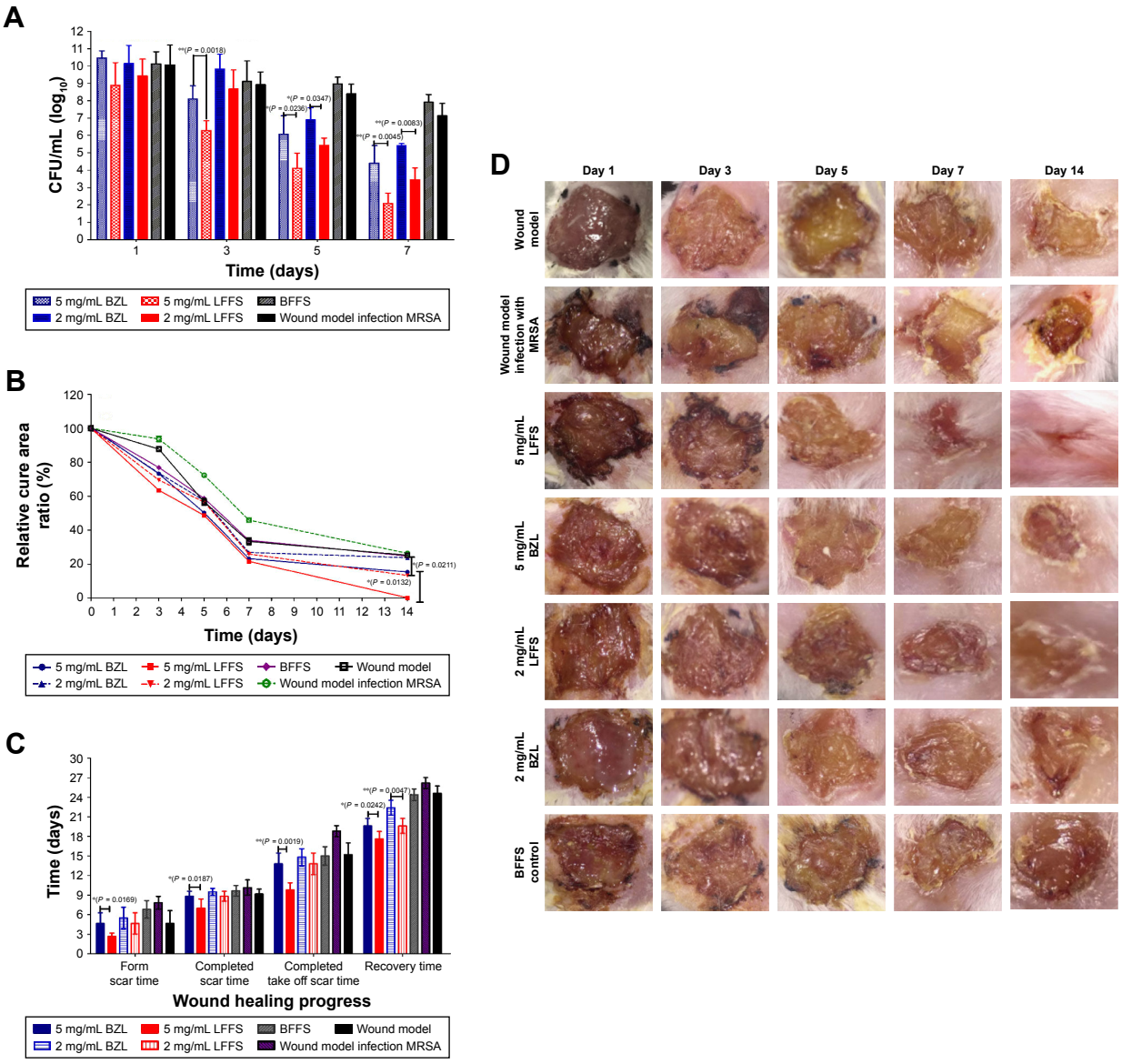

Figure 4 Antibacterial activity against MRSA in vivo. (**A**) Viable bacterial count of the wound. (**B**) Relative cure area ratio of the wound. (**C**) Wound-healing progress. (**D**) Graphical illustration of the changes in wound size on days 1, 3, 5, 7, and 14.

Notes: $^{**}P < 0.01$ denotes a highly significant difference, and $^{*}P < 0.05$ denotes a significant difference (n = 6).

Abbreviations: BFFS, blank film-forming system; BZL, benzalkonium bromide; MRSA, methicillin-resistant *Staphylococcus aureus*.

and 76.29% were observed in the 5 mg/mL BZL, 2 mg/mL LFFS, and 2 mg/mL BZL treated, respectively.

In Figure 4C, the scar formation time and complete scar time after treatment with 5 mg/mL LFFS were 2.66 ± 0.51 days and 7.0 ± 1.41 days, respectively, while the corresponding values for wounds treated with 5 mg/mL BZL were 4.66 ± 1.63 days and 8.83 ± 0.75 days. The scar formation time and complete scar time of LFFS treatment were 1.75 times and 1.26 times shorter than those for BZL treatment, respectively ($P = 0.0169$; $P = 0.0187$). The time required for complete scar disappearance and the recovery time for wounds treated with 5 mg/mL LFFS were 9.8 ± 1.09 days and 17.6 ± 1.14 days, respectively, and the corresponding values for wounds treated with 5 mg/mL were 13.8 ± 1.64 days and 19.61 ± 1.14 days, which were 1.40 times and 1.11 times longer, respectively, than those observed with LFFS treatment ($P = 0.0019$; $P = 0.0242$).

The wound size on day 3 after treatment with 5 mg/mL and 2 mg/mL LFFS was noticeably reduced compared with that of wounds treated with the negative control and BZL, as shown in Figure 4D. The wound size in the LFFS-treated groups was significantly reduced compared with that in the negative control group on days 5 and 7. The wound closure rate was greatly accelerated with the 5 mg/mL LFFS treatment. On day 14, complete wound healing was observed in the 5 mg/mL LFFS treatment group. In summary, LFFS treatment for wounded skin exhibited satisfactory bactericidal power against MRSA252 and improved wound-healing activity.

Anti-biofilm inhibitory and clearance activity

Crystal violet staining

The OD value at 570 nm of specimens treated with BZL at 1.33 μg/mL for 24 hours was 1.983 ± 0.112 and that of specimens treated with the LFFS was 0.574 ± 0.178 (three times higher than BZL, $P = 0.0001$), as shown in the Figure S5A. The OD value at 570 nm of samples treated with 5 mg/mL BZL for 8 hours was 1.873 ± 0.095, a value nearly 1.57 times larger than that of samples treated with the LFFS (1.191 ± 0.032, $P = 0.0003$), as shown in Figure S5B. These data showed that the LFFS has stronger inhibitory and clearance activity than BZL.

Biofilm surface construction after inhibition and clearance

The biofilms of bacteria treated with 1.33 μg/mL LFFS for 24 hours (Figure 5A) appeared spread out and damaged,

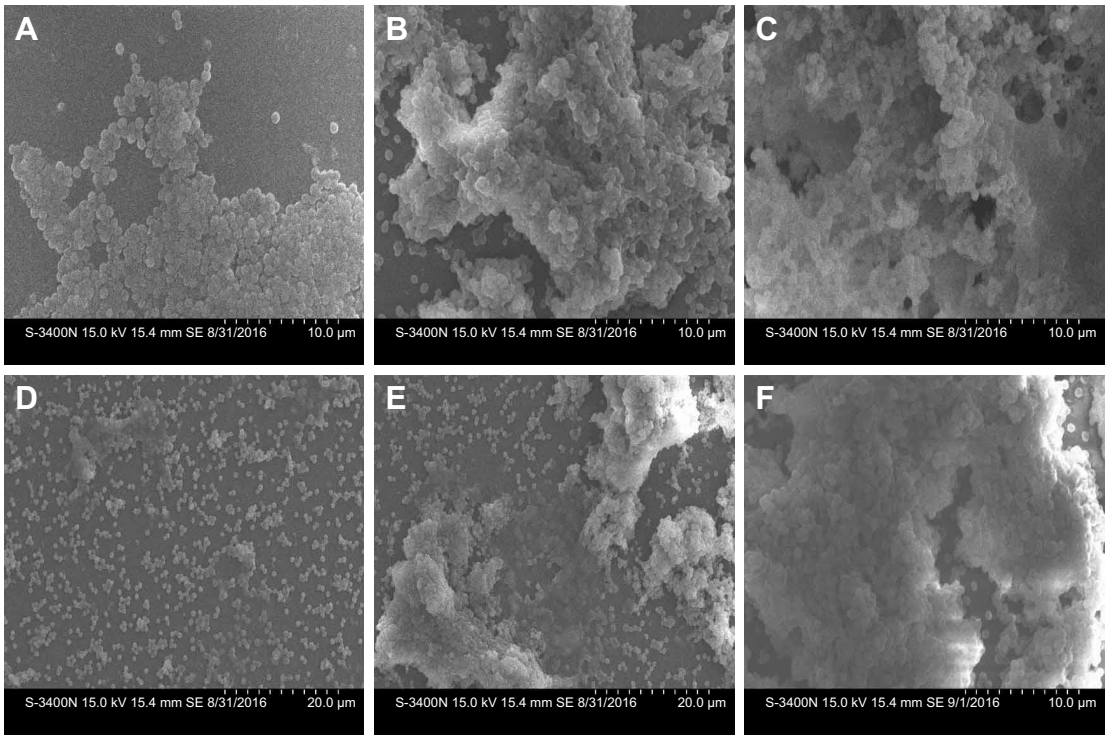

Figure 5 Biofilm surface structure after inhibition and clearance by SEM. (**A** and **B**) Groups treated with 1.33 μg/mL LFFS and BZL (magnification 4000×) (**C**) BFFS group (×15.4 μm, 4,000×). (**D** and **E**) Groups treated with 5 mg/mL LFFS and BZL (magnification 4000×). (**F**) MRSA control (magnification 4000×).
Abbreviations: BFFS, blank film-forming system; BZL, benzalkonium bromide; LFFS, liquid film-forming system; MRSA, methicillin-resistant *Staphylococcus aureus*; SEM, scanning electron microscope.

and the amount of bacteria present was distinctly decreased. In contrast, the MRSA biofilms treated with BZL at an identical concentration (Figure 5B) were only mildly affected. The biofilms were dense, and the bacteria appeared normal after BFFS treatment (Figure 5C). Similarly, Figure 5D shows that after exposure to 5 mg/mL LFFS for 8 hours, the biofilm structure was scattered and damaged. In addition, the bacterial cell clusters treated with LFFS had a much lower thickness than those exposed to BZL at the same density (Figure 5E). Overall, these results show that LFFS has a much stronger influence on the biofilm clearance and its formation inhibition than BZL.

CLSM imaging of biofilm formation and removal

Green fluorescence indicated living bacteria, and red fluorescence indicated dead bacteria (Figure 6A–F). LFFS treatment of 1.33 μg/m significantly increased the proportion of dead cells within biofilms (Figure 6A–C). Living bacteria and dead/living bacteria after treatment with BZL accounted for 89.206% ± 1.892% and 12.134% ± 2.406% of all bacteria, respectively, which were 2.10 times and 11.288 times higher than those after treatment with LFFS-treated samples 42.347% ± 3.031% and 136.98% ± 17.581% ($P = 0.0001$), as shown in the Figure S6A. Importantly, the red fluorescence in samples treated with 5 mg/mL LFFS for 8 hours was primarily spread throughout entire field of view, while green fluorescence was scarcely observed on the horizon (Figure 6D). In contrast, the green fluorescence area in samples treated with BZL covered nearly the entire horizon, whereas red fluorescence appeared in a small area (Figure 6E). Figure S6B showed that 85.882% ± 2.880% live bacteria and 121.364% ± 15.868% dead/living bacteria after treatment with BZL, whereas the corresponding values for the LFFS-treated samples were 45.33% ± 3.258% and 16.526% ± 3.913%, which were 1.894 times and 7.34 times higher than those for BZL, as shown in Figure S6B ($P = 0.0001$; $P = 0.0001$). Therefore, the LFFS was clearly more effective in biofilm clearance than BZL.

Inspecting the inhibition and removal of 3D biofilm constructions by AFM

The average height of MRSA biofilms treated with 1.33 μg/mL BZL for 24 hours was larger than that of those treated with the LFFS at the same concentration and time (Figure 7A, B, E, and F). The mean height of the remaining biofilms treated with 5 mg/mL BZL for 8 hours was also greater than that of the biofilms treated with the LFFS at the same concentration and for the same amount of time (Figure 7C, D, G, and H). In addition, the Ra, Rq, Rz, Rku, and Rsk values of biofilms treated with 1.33 mg/mL or 5 mg/mL BZL were larger than those of biofilms treated with the LFFS (Figure S7A–D). Clearly, the biofilm removal efficacy competence for biofilms of BZL is mildly less than that of the LFFS at same

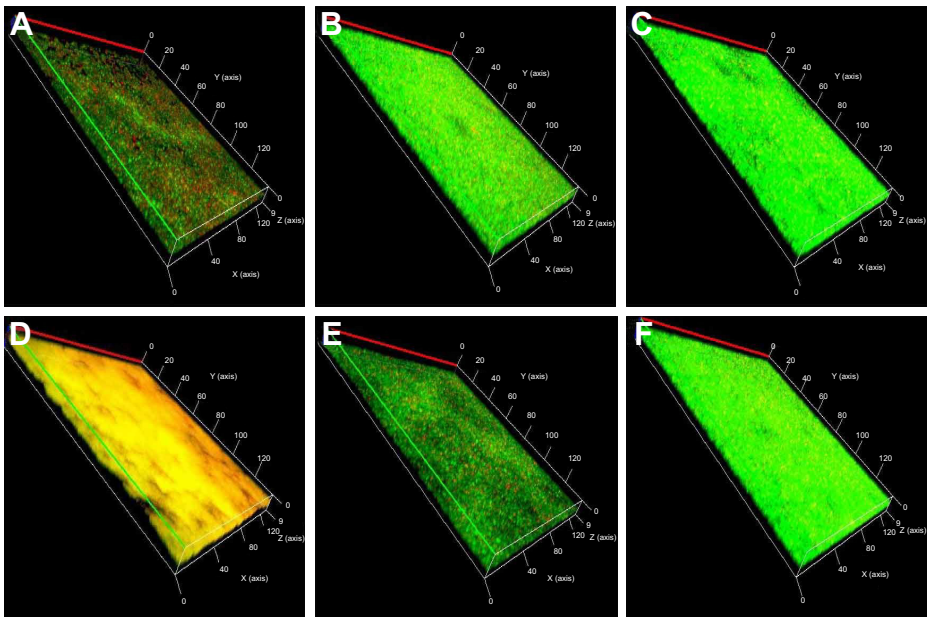

Figure 6 CLSM micrographs of biofilm structure after inhibition and clearance. (**A** and **B**) Groups treated with 1.33 μg/mL LFFS and BZL. (**C**) BFFS control group. (**D** and **E**) Groups treated with 5 mg/mL LFFS and BZL LFFS. (**F**) MRSA control group.

Abbreviations: BFFS, blank film-forming system; BZL, benzalkonium bromide; CLSM, confocal laser scanning microscope; LFFS, liquid film-forming system; MRSA, methicillin-resistant *Staphylococcus aureus*.

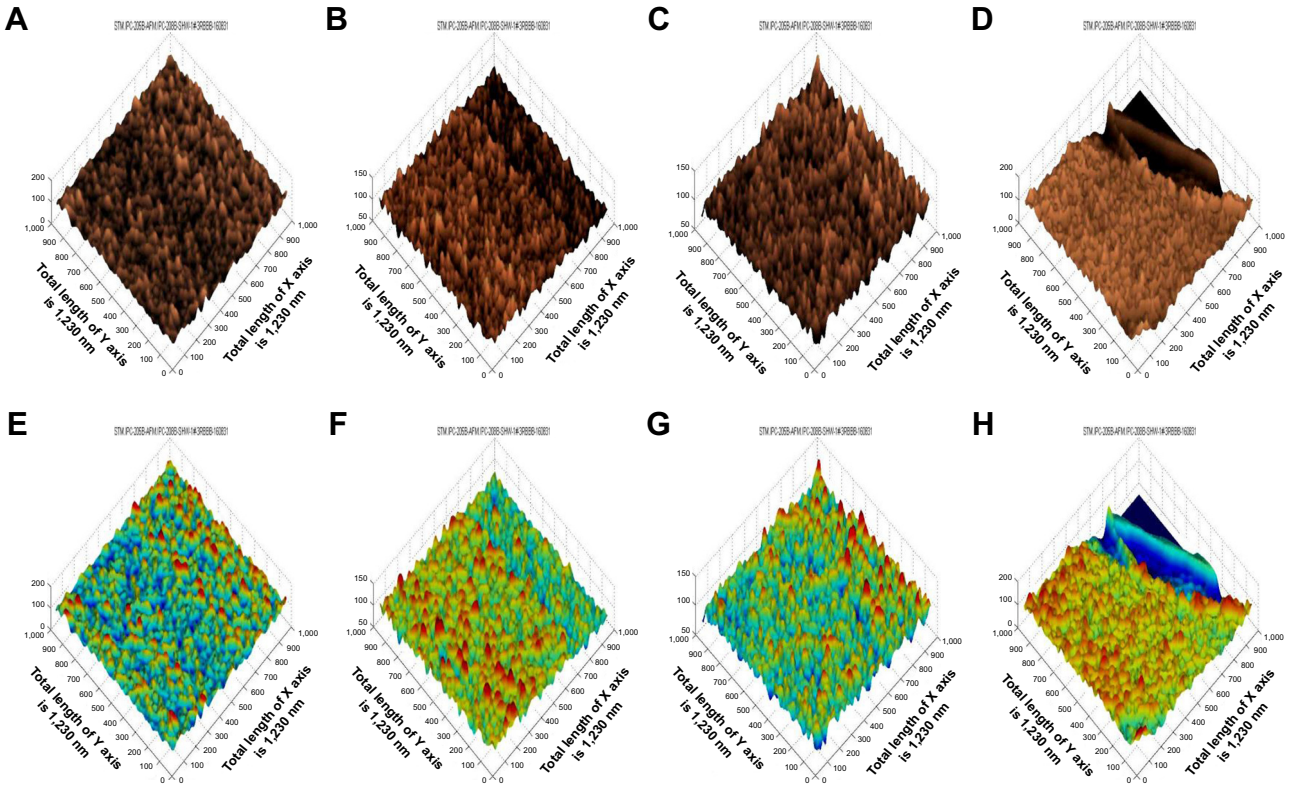

Figure 7 Biofilm 3D structures of inhibition and clearance by AFM (**A** and **C**). Grayscale image after treatment with 1.33 μg/mL and 5 mg/mL LFFS. (**B** and **D**) Grayscale figure after treated with 1.33 μg/mL and 5 mg/mL of BZL. (**E** and **G**) Color image after treatment with 1.33 μg/mL and 5 mg/mL LFFS. (**F** and **H**) Color image after treatment with 1.33 μg/mL and 5 mg/mL BZL.
Abbreviations: 3D, three dimensional; AFM, atomic force microscope; BZL, benzalkonium bromide; LFFS, liquid film-forming system.

density for the identical time. Thus, the restriction of biofilm formation by BZL was weaker than that by the LFFS after latency at equivalent concentrations and for equivalent lengths of times.

Cell and membrane damage by the LFFS

Effect of BZL on MRSA cell morphology

After exposure to 1.33 μg/mL BZL for 24 h at 40× and 60× (Figure 8A and B), most MRSA cells exhibited complete and recognizable cytomembranes with consistently allocated cytosol and electron concentrations within most cells in general. In contrast, MRSA cells treated with the LFFS at the same concentration displayed changed and damaged cytomembranes under the above times (Figure 8C and D). Their cytoplasm membranes were partially separated from the cell wall, thus, resulting in large vacuoles enclosing the cytoderm. Additionally, the cytoplasm of MRSA cells treated with the LFFS shrank and the electron concentrations were unevenly allocated within these cells. The cells displayed abnormal shapes, and portions of their cell wall were cracked, thus resulting in release of their components, for example, proteins, electrolytes, nucleic acids, and intracellular enzymes. The infiltration of this film together with the cell wall transformation regarding the penetrability of the cytomembranes may have led to the abovementioned variations.

Integrity of the bacterial cell wall

Figure 9A shows that alkaline phosphate (AKP) release discharge proceeded as a function of over time; however, clear differences were observed in AKP release between divulgation in cells treated with the LFFS and BZL. After 2 and 4 hours, the amount of AKP released from cells treated with LFFS was 4.50 ± 0.763 U/L and 6.567 ± 0.854 U/L, respectively, which were 1.92- and 2.384-fold higher than that released from cells treated with BZL (2.33 ± 0.577 U/L, 2.753 ± 0.873 U/L) ($P = 0.0243$; $P = 0.0068$). Thus, these results showed that the LFFS was more effective in destroying the cell wall than BZL.

Integrity of the bacterial cytomembranes

The OD values at 260 nm and 280 nm after 1.33 μg/mL LFFS treatment were 1.408 ± 0.08 and 0.847 ± 0.057, respectively (Figure 9B). However, for 1.33 μg/mL BZL

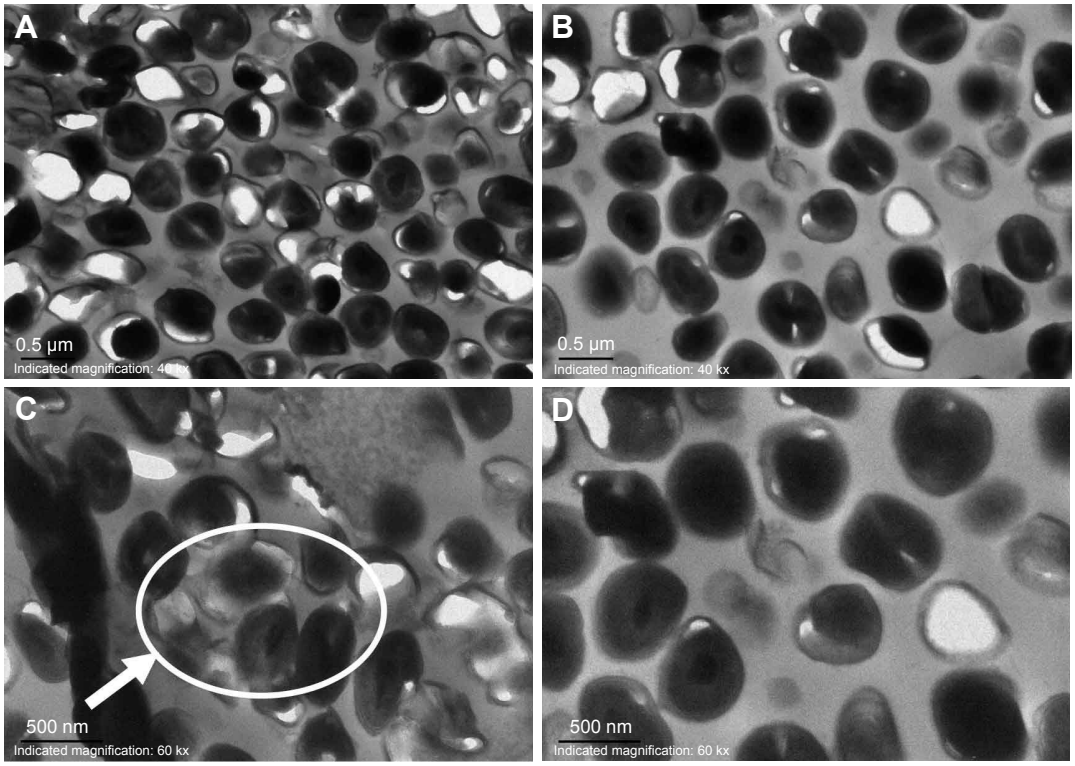

Figure 8 Cell membrane structural damage observed by TEM: (**A** and **B**) LFFS- and BZL-treated group at 40,000× magnification. (**C** and **D**) LFFS- and BZL-treated group at 60,000× magnification. The area within the oval circle indicate by the white arrow show the damaged cytomembranes of MRSA.
Abbreviations: BZL, benzalkonium bromide; LFFS, liquid film-forming system; TEM, transmission electron microscopy.

treatment, the OD at 260 nm was 0.450 ± 0.027, and the OD at 280 nm was 0.039 ± 0.042. The OD_{260} and OD_{280} of the LFFS-treated samples were 1.663- and 1.142-fold larger than those of the BZL-treated samples, respectively ($P = 0.0001$; $P = 0.0004$). Additionally, the LDH release level was time dependent, but clear differences were observed between samples treated with the LFFS and BZL (Figure 9C). After 2 and 4 hours, the level of LDH released from cells treated with the LFFS was 29.172 ± 13.134 U/L and 46.642 ± 1.224 U/L, respectively, which were 3.097 times and 2.231 times greater than that released from cells treated with BZL (9.42 ± 3.03 U/L and 20.908 ± 4.526 U/L) after 2 and 4 hours ($P = 0.0262$; $P = 0.0076$). As a result, irreversible disruption of the cytoplasmic membranes is likely, and thus results in the leakage of cell components and cell death.

Cell membrane permeability

At both 2 and 4 hours, the relative electrical conductivity ratios for samples treated with 1.33 μg/mL LFFS were significantly higher than those for samples treated with BZL for both 2 and 4 hours (Figure 9D). Compared with that of BZL-treated samples, the relative electrical conductivity in MRSA cell suspensions treated with LFFS increased more directly and quickly. The K^+ and Mg^{2+} concentrations of MRSA treated with the LFFS were obviously higher than those in MRSA treated with BZL for both 2 and 4 hours (Figure 9E and F). Thus, the penetrability of the bacterial membranes can be relatively increased, thereby leading to the release of the intracellular components and, in particular, decreasing the concentrations of electrolytes such as K^+ and Mg^{2+}.

Discussion

As a major health problem globally, wounds place great burdens on patients and health care systems. In 2012, 7.5% of American patients who underwent surgical resection for cancer suffered from wounds.[17] Wound healing refers to a complex cascade of cellular events involving four intricate and overlapping phases: hemostasis, inflammation, proliferation, and tissue remodeling.[18] Many factors influence wound healing, such as the location of the wound and concomitant diseases.[19] In open wounds, bacteria are common and key problem in delayed healing and increasing the risks of morbidity. In South Africa and Asia Pacific, 15% of wound infections are due to MRSA.[20] Thus, the dissemination of best practices to prevent wounds is vital. Therefore, we chose a second-degree skin wound model with MRSA infection as our research objective.

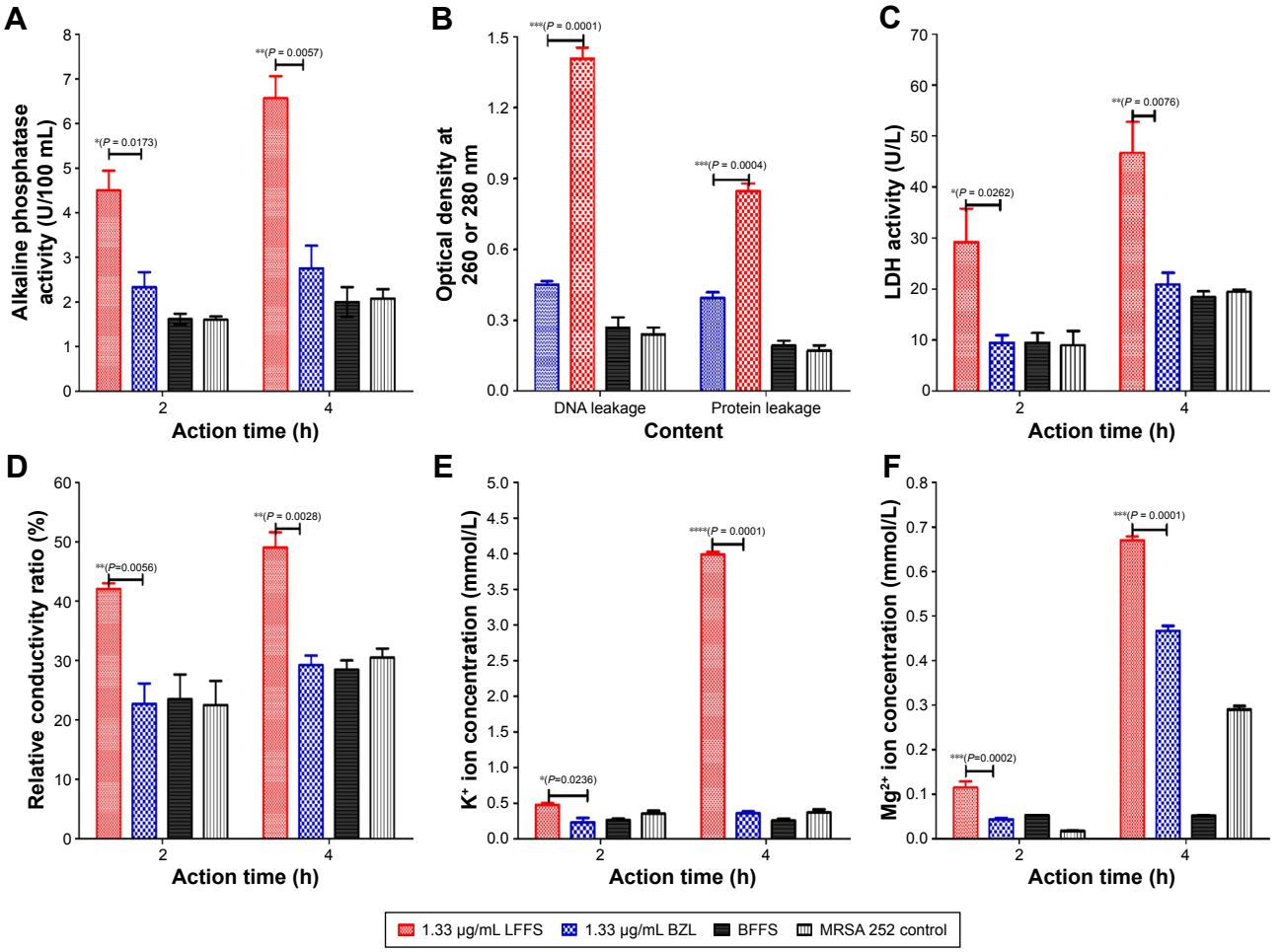

Figure 9 Cell and membrane damage integrity. (**A**) AKP activity of bacteria. (**B**) OD of the suspension at 260 nm and 280 nm. (**C**) LDH activity. (**D**) Relative conductivity ratio (%) of the bacterial suspension. (**E** and **F**) Concentration of K^+ and Mg^{2+} ions in the bacterial suspension.

Notes: ***$P < 0.001$ represents an extremely significant difference, **$P < 0.01$ represents a highly significant difference, and *$P < 0.05$ represents a significant difference (n = 3). ****$P<0.0001$.

Abbreviations: AKP, alkaline phosphate; BFFS, blank film-forming system; BZL, benzalkonium bromide; LDH, lactate dehydrogenase; OD, optical density.

It is well known that PVA can be used to improve the strength, water resistance, and thermal stability of films.[21] Its concentration is a key factor in forming film system. According to our previous studies, systems with PVA concentrations less than 10% can form good films. Therefore, we designed a novel LFFS with five PVA. The results shown that F7 (LFFS with 5% PVA) had an incompact and asymmetric morphology that created larger pores with an irregular shape. Additionally, F7 has a different blocky and straticulate structure from the LFFSs with other PVA concentrations (Figure S1C and H). Moreover, F7 displayed good stability and a delayed release profile in PBS at different pH values (pH 4.0, 6.0, and 8.0) in vitro (Figure S2). We found that reaching 90% release from BZL solution took 45 minutes, while F7 reached 90% release at 72, 72, and 90 hours at pH 4.0, 6.0, and 8.0, respectively. Importantly, the LFFS displayed a powerful antibacterial effect against MRSA 252 (Table S2, Figure 2B and C). Therefore, we chose LFFS prepared with the 5% PVA.

In this study, we found that both the MIC and MBC values of BZL (both 5.0 μg/mL) were 3.49-fold higher than those of the LFFS (both 1.43 μg/mL). The time-killer assay showed that the LFFS has good efficacy and is a fast-acting bactericide. Importantly, we also find that the LFFS at both 2 and 5 mg/mL has stronger and faster action against the MRSA-infected skin wound model regarding the three main indexes (rapid wound healing, viable bacterial counts, and rapid wound progress) than the same concentrations of BZL. These data have also confirmed that LFFS has about an approximately four times stronger bactericidal effect against MRSA than BZL aqueous solution in vivo and in vitro.

The LFFS exerted a stronger and more rapid bactericidal effect against MRSA than BZL solution both in vivo and in vitro. We consider the LFFS as a promising material for

the following reasons. First, wound dressing materials and advanced products have been developed for protecting skin and improving healing ability.[17] Additionally, wound-healing materials need a swelling capability to absorb excess exudates, need oxygen permeability to permit respiration, and need the ability to eliminate of infection,[22] all of which are met by the LFFS, indicating its potential to promote wound healing. Second, the ability of LFFS to absorb BZL is essential for maintaining its antibacterial properties. BZL is also used in the treatment and prevention of wound infections, particularly those open wounds associated with bacterial infection.[23] Finally, BZL is widely applied in health care and utilized daily in disinfectant and cleaning products, baby lotions, nasal decongestants, sun creams, pain relief treatments, mouthwashes, and toothpastes.[12] Therefore, the LFFS exerted a strong bactericidal effect against MRSA.

Biofilms are a major factor in delayed wound healing. Many steps are involved in biofilm formation, including the presence of a favorable substrate presence, cell deposition, attachment and desorption, cell-to-cell signaling, detachment, and growth.[24] The quality and structure of the biofilm determine its resistance to a variety of antimicrobials agents; therefore, a reduction in and inhibition of the sensitivity of MRSA biofilms is observed. Our results demonstrate that treatment with LFFS at 1.33 μg/mL (which inhibits biofilm formation) and 5 mg/mL (which clears biofilms) are more effective than the same concentration of BZL based on by the crystal violet staining, SEM, AFM, and CLSM (Figures 5–7 and S5–S7).

Membranes and cell walls are crucial to the survival of bacteria. In this study, we found that the LFFS has a stronger ability to damage cell membranes than BZL at equivalent concentrations; however, the cell wall structure was not damaged by either the LFFS or BZL. Furthermore, we found that the level of AKP released from MRSA cells was greater after LFFS treatment, indicating that LFFS can cause cytoplasmic leakage from MRSA. Importantly, changes in DNA, proteins, electrical conductivity, and K^+ and Mg^{2+} concentrations are important indicators of membrane damage in bacteria, and changes due to membrane perturbation can induce cell death.[25] Our results showed that the LFFS had a stronger ability to disrupt the bacterial cell membrane structure and induce cytoplasmic leakage than BZL. There is no obvious toxicity, such as death, bleeding, pebbling, or skin irritation, at the wound site during the LFFS for consecutive 14 days twice a day. The LFFS and its excipients had no obvious cell toxicity at the tested concentrations, and other formulations with the active drug substance had similar toxicity to that observed in L929 cells treated with 3.91 μg/mL BZL for 24 hours according to the ISO 10993-5:1999 (Part 5: Tests for in vitro cytotoxicity standard). However, some questions related to alternative wound models and topical pharmacokinetics still require further research. Overall, our results demonstrate that this novel LFFS is a promising antimicrobial agent's delivery system with considerable potential for use in treating MRSA wound infections.

Acknowledgments

This study was supported by the National Major Scientific and Technological Special Project for "Significant New Drugs Development" (number 2016ZX09J16102-002), the National Natural Science Foundation of China (number 31670938), and the Natural Science Foundation Project program of Chongqing CSTC (number 2014jcyjA10107).

Disclosure

The authors report no conflicts of interest in this work.

References

1. Ramasamy P, Shanmugam A. Characterization and wound healing property of collagen-chitosan film from Sepia kobiensis (Hoyle, 1885). *Int J Biol Macromol*. 2015;74:93–102.
2. Agostinho AM, Hartman A, Lipp C, Parker AE, Stewart PS, James GA. An in vitro model for the growth and analysis of chronic wound MRSA biofilms. *J Appl Microbiol*. 2011;111(5):1275–1282.
3. Das S, Baker AB. Biomaterials and nanotherapeutics for enhancing skin wound healing. *Front Bioeng Biotechnol*. 2016;4:82.
4. Sarhan WA, Azzazy HM, El-Sherbiny IM. Honey/chitosan nanofiber wound dressing enriched with allium sativum and cleome droserifolia: enhanced antimicrobial and wound healing activity. *ACS Appl Mater Interfaces*. 2016;8(10):6379–6390.
5. Kim JY, Jun JH, Kim SJ, et al. Wound healing efficacy of a chitosan-based film-forming gel containing tyrothricin in various rat wound models. *Arch Pharm Res*. 2015;38(2):229–238.
6. Beck ET, Buchan BW, Reymann GC, Ledeboer NA, McAdam AJ. Comparison of ESwab and wound fiber swab specimen collection devices for use with Xpert SA nasal complete assay. *J Clin Microbiol*. 2016;54(7):1904–1906.
7. Dou JL, Jiang YW, Xie JQ, Zhang XG. New is old, and old is new: recent advances in antibiotic-based, antibiotic-free and ethnomedical treatments against methicillin-resistant *Staphylococcus aureus* wound infections. *Int J Mol Sci*. 2016;17(5):pii:E617.
8. Liu YH, Wu HJ, Ma WX. Spectrophotometric determination of benzalkonium bromide in pharmaceutical samples with alizarin green. *J Surfactants Deterg*. 2013;16(2):265–269.
9. Smith JK, Bumgardner JD, Courtney HS, Smeltzer MS, Haggard WO. Antibiotic-loaded chitosan film for infection prevention: a preliminary in vitro characterization. *J Biomed Mater Res B Appl Biomater*. 2010;94(1):203–211.
10. Suktham K, Koobkokkruad T, Saesoo S, Saengkrit N, Surassmo S. Physical and biological characterization of sericin-loaded copolymer liposomes stabilized by polyvinyl alcohol. *Colloids Surf B Biointerfaces*. 2016;148:487–495.
11. Huang YC, Chu HW, Huang CC, Wu WC, Tsai JS. Alkali-treated konjac glucomannan film as a novel wound dressing. *Carbohydr Polym*. 2015;117:778–787.

12. Lukáč M, Mrva M, Garajová M, et al. Synthesis, self-aggregation and biological properties of alkylphosphocholine and alkylphosphohomocholine derivatives of cetyltrimethylammonium bromide, cetylpyridinium bromide, benzalkonium bromide (C16) and benzethonium chloride. *Eur J Med Chem*. 2013;66:46–55.
13. Yang Y, Li H, Sun H, et al. A novel nitro-dexamethasone inhibits agr system activity and improves therapeutic effects in MRSA sepsis models without antibiotics. *Sci Rep*. 2016;6:20307.
14. Kurabayashi H, Tamura K, Machida I, Kubota K. Inhibiting bacteria and skin pH in hemiplegia. *Am J Phys Med Rehabil*. 2002;81(1):40–46.
15. Schneider LA, Korber A, Grabbe S, Dissemond J. Influence of pH on wound-healing: a new perspective for wound-therapy? *Arch Dermatol Res*. 2007;298(9):413–420.
16. Song Z, Sun H, Yang Y, et al. Enhanced efficacy and anti-biofilm activity of novel nanoemulsions against skin burn wound multi-drug resistant MRSA infections. *Nanomedicine*. 2016;12(6):1543–1555.
17. Yang S, Park J, Lee H, et al. Sequential change of wound calculated by image analysis using a color patch method during a secondary intention healing. *PLoS One*. 2016;11(9):e0163092.
18. Hobson R. Vitamin E and wound healing: an evidence-based review. *Int Wound J*. 2016;13(3):331–335.
19. Pereira RF, Bártolo PJ. Traditional therapies for skin wound healing. *Adv Wound Care (New Rochelle)*. 2016;5(5):208–229.
20. Dodds TJ, Hawke CI. Linezolid versus vancomycin for MRSA skin and soft tissue infections (systematic review and meta-analysis). *ANZ J Surg*. 2009;79(9):629–635.
21. Hajji S, Chaker A, Jridi M, et al. Structural analysis, and antioxidant and antibacterial properties of chitosan-poly (vinyl alcohol) biodegradable films. *Environ Sci Pollut Res Int*. 2016;23(15):15310–15320.
22. Ranjbar-Mohammadi M, Rabbani S, Bahrami SH, Joghataei MT, Moayer F. Antibacterial performance and in vivo diabetic wound healing of curcumin loaded gum tragacanth/poly(epsilon-caprolactone) electrospun nanofibers. *Mater Sci Eng C Mater Biol Appl*. 2016;69:1183–1191.
23. Xu R, Zhang L, Zhao X, et al. Benzalkonium bromide as a new potential instillation drug for bladder cancer: hypothesis and pilot study. *Med Sci Monit*. 2011;17(12):HY36–HY39.
24. Li YF, Sun HW, Gao R, et al. Inhibited biofilm formation and improved antibacterial activity of a novel nanoemulsion against cariogenic Streptococcus mutans in vitro and in vivo. *Int J Nanomedicine*. 2015;10(1):447–462.
25. Castillo JA, Clapés P, Infante MR, Comas J, Manresa A. Comparative study of the antimicrobial activity of bis(Nalpha-caproyl-L-arginine)-1,3-propanediamine dihydrochloride and chlorhexidine dihydrochloride against *Staphylococcus aureus* and *Escherichia coli*. *J Antimicrob Chemother*. 2006;57(4):691–698.